

Two-dimensional hexagonal FeX_2 ($\text{X}=\text{Cl}, \text{Br}, \text{I}$) monolayers: magnetism, electronic structures and light-induced chiral edge states

Xiangru Kong,^{1,2,3} Linyang Li,^{4,5,*} Liangbo Liang,³ François M. Peeters,⁵ and Xiong-Jun Liu^{1,2,6,7}

¹International Center for Quantum Materials and School of Physics, Peking University, Beijing 100871, China

²Collaborative Innovation Center of Quantum Matter, Beijing 100871, China.

³Center for Nanophase Materials Sciences, Oak Ridge National Laboratory, Oak Ridge, Tennessee 37831, United States

⁴School of Science, Hebei University of Technology, Tianjin 300401, China

⁵Department of Physics, University of Antwerp, Groenenborgerlaan 171, B-2020 Antwerp, Belgium

⁶Beijing Academy of Quantum Information Science, Beijing 100193, China

⁷CAS Center for Excellence in Topological Quantum Computation, University of Chinese Academy of Sciences, Beijing 100190, China

Topological materials are fertile ground for investigating topological phases of matter and topological phase transitions. In particular, the quest for novel topological phases in 2D materials is attracting fast growing attention. Here, using Floquet-Bloch theory, we propose to realize chiral topological phases in 2D hexagonal FeX_2 ($\text{X}=\text{Cl}, \text{Br}, \text{I}$) monolayers under irradiation of circularly polarized light. Such 2D FeX_2 monolayers are predicted to be dynamical stable, and exhibit both ferromagnetic and semiconducting properties. To capture the full topological physics of the magnetic semiconductor under periodic driving, we adopt *ab initio* Wannier-based tight-binding methods for the Floquet-Bloch bands, with the light-induced band gap closings and openings being obtained as the light field strength increases. The calculations of slab with open boundaries show the existence of chiral edge states which are robust to disorders. Interestingly, the topological transitions with branches of chiral edge states changing from zero to one and from one to two by tuning the light amplitude are obtained, showing that the topological Floquet phase of high Chern number can be induced in the present Floquet-Bloch systems.

I. INTRODUCTION

The discovery of the integer quantum Hall (QH) effect [1], which is characterized by topological Chern number [2], brought about the new fundamental notion of topological quantum phases. The topological phases are now a mainstream of research in condensed matter physics, with the research being greatly revived after the discovery of topological insulators [3–6]. Among the topological phases, the magnetic topological materials are of peculiar interests. In particular, the quantum anomalous Hall (QAH) effect, the version of QH effect without Landau levels and first proposed by Haldane [7], was first realized in experiment by in a thin film magnetic topological insulator [8]. The magnetic topological materials with robust topological edge states have the potential application for future nanodevices [9–11]. Moreover, the chiral topological superconductivity with chiral Majorana modes was reported based on QAH phases in proximity of an *s*-wave superconductor [12]. The Majorana zero modes in topological superconductor can obey non-Abelian statistics and have important potential applications to topological quantum computation [13–16], and thus have also attracted considerable interests.

Nevertheless, the magnetic materials are rare in comparison with nonmagnetic materials [17, 18]. Magnetic materials are the major platform for spintronics [19], and the controllability of the spin degree of electrons depends

on the material dimension [20, 21]. On the other hand, due to the discovery of graphene [22–24], two-dimensional (2D) atomic like materials have attracted great interests. Many 2D materials have been studied such as elemental group IV or V monolayers [24–26] and transition metal dichalcogenide (TMD) monolayers [27–29]. To realize spintronics in 2D materials, a typical way is to dope magnetic elements [17], which however has the disadvantage in leading to disorders. In comparison, due to the partially filled *d* sub-shell in transition metals [30], the intrinsic magnetic semiconductors may be realized in 2D TMD or other similar transition metal compounds such as transition metal halides.

Another important issue is how to manipulate the topological quantum phase. Despite a large amount of 2D topological materials that have been predicted [9, 10], controlling topological phase transitions usually require changing the structural properties of materials [31–33]. Recently, the non-equilibrium schemes for topological phases, including the quantum quenches [34] and periodic driving by optical pumping with time-dependent perturbations [35–37], enable the non-equilibrium manipulations of topological quantum phases and attracted fast growing attention. The first proposal for Floquet topological insulators was realized in HgTe/CdTe quantum wells [38]. In experiments, Floquet-Bloch states were observed on the surface of topological insulators [36, 37]. Due to the existence of electronic valley degree of freedom in TMD [39], It is interesting to investigate Floquet physics in TMD [35, 40, 41], and study the topological phases in magnetic semiconducting transition metal compounds by Floquet-Bloch theory [42–47].

* linyang.li@hebut.edu.cn

In this work, after showing that hexagonal (2H) FeX_2 ($\text{X}=\text{Cl}, \text{Br}, \text{I}$) monolayers are ferromagnetic semiconductors, which are dynamically stable, we propose to realize and control the topological phases in FeX_2 by coupling it to circularly polarized light. For the present Floquet-Bloch states, instead of using a simple band description which may fail, we use *ab initio* Wannier-based tight-binding methods for calculating the Floquet-Bloch band structures and the light-induced chiral edge states. Different Floquet topological states with high Chern number are obtained by controlling the strength of the light field, showing the intriguing controllability of the present topological matter.

II. COMPUTATIONAL METHODS

First-principles calculations were implemented in the Vienna *ab initio* simulation package (VASP) with projector augmented wave (PAW) method [48, 49] in the framework of Density Functional Theory (DFT) [50]. The electron exchange-correlation functional was adopted as the generalized gradient approximation (GGA) in the form proposed by Perdew, Burke and Ernzerhof (PBE) [51]. The structural relaxation considering both the atomic positions and lattice vectors was performed by using the conjugate gradient (CG) scheme until the maximum force on each atom was less than $0.01 \text{ eV}/\text{\AA}$, and the total energy is converged to 10^{-5} eV . The energy cutoff of the plane waves was chosen as 520 eV . The Brillouin zone (BZ) integration was sampled by using a Γ -centered $21 \times 21 \times 1$ Monkhorst-Pack grid. Phonon frequencies were calculated by the finite displacement method with the *Phonopy* code [52]. The Floquet-Bloch band structures, slab and surface state calculations were illustrated with *ab initio* Wannier-based tight-binding methods [53, 54]. The iterative Greens function method was used for surface state calculations [55].

III. RESULTS

The hexagonal (2H) FeX_2 ($\text{X}=\text{Cl}, \text{Br}, \text{I}$) monolayers possess the point group C_{3h} with broken inversion symmetry, which is the same as in 2H TMD monolayers [27, 28]. Honeycomb structures are shown from the top view (Fig. 1(a)), and sandwich-like stacking of atom layers (X-Fe-X) are observed from the side view (Fig. 1(b)). Recently, the triangular (1T) FeX_2 monolayers were predicted to exhibit ferromagnetic (FM) ground state with metallic electronic properties [56, 57]. Here, we investigate the magnetic ground states of 2H FeX_2 monolayers by constructing a $2 \times 2 \times 1$ supercell. Three magnetic configurations are considered as shown in Fig. 1(c): FM, AFM1, AFM2. The energy calculations indicate that the magnetic ground state of 2H FeX_2 monolayers is FM. Take FeI_2 for example, the energy of FM state is about 125 meV per Fe atom lower than that of

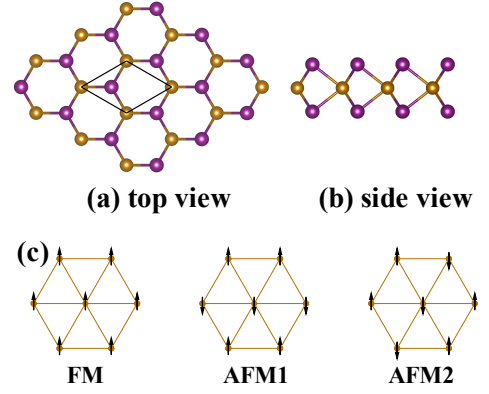


FIG. 1. The lattice structure of FeX_2 : (a) top view and (b) side view. (c) Three magnetic configurations: FM, AFM1, AFM2. The golden symbols indicate the Fe atom, and the purple symbols refer to the halogen atom ($\text{X}=\text{Cl}, \text{Br}, \text{I}$). FM = ferromagnetic, AFM = antiferromagnetic.

the AFM1 state, and about 159 meV per Fe atom lower than that of the AFM2 state. The Fe ($3d^6 4s^2$) atom donates one electron for each halogen atom ($\text{X}=\text{Cl}, \text{Br}, \text{I}$) such that the new electron configuration of Fe atom becomes $3d^4 4s^2$, and the four electrons in the d orbital will form $\uparrow\uparrow\uparrow$ spin configuration. DFT calculations confirm that the total magnetization of the 2H FeX_2 monolayers in the unit cell is $4 \mu_B$. By noncollinear magnetic calculations, the easy magnetic axis of 2H FeX_2 is in-plane, and the Magnetocrystalline Anisotropy Energy (MAE) of the out-of-plane spin orientation which can be aligned by magnetic field is about 1.1 meV per spin for every Fe atom. To demonstrate the dynamical stability of FM 2H FeX_2 monolayers, the phonon spectrum without imaginary frequency modes are shown in Fig. S1 in the supporting information (SI).

Here, we consider the electronic band structures of FeX_2 monolayers for collinear magnetic state, i.e., without spin-orbit coupling (SOC), and noncollinear magnetic state (with SOC, in-plane and out of plane magnetization). The collinear magnetic state of FeI_2 exhibits spin-polarized bands as shown in Fig. 2(a), and similar for FeCl_2 in Fig. S2 and FeBr_2 in Fig. S3. The bands near the Fermi level consists mostly of transition-metal d -orbitals, which could be split into three groups, $d_{3z^2-r^2}$, $d_{x^2-y^2} \pm id_{2xy}$ and $d_{xz} \pm id_{yz}$ as based on the symmetry analysis as shown in Figs. 2(b) and (c) (also see Figs. S2 and S3) [35]. As the electronegativity of halogen atoms (Cl, Br, I) decrease, the lattice constants (a), the height (h) and the Fe-X bond length (d) of the FeX_2 monolayer increase (see Table I). This results in weaker repulsive interaction between the d orbitals of the Fe atoms, and consequently the band gaps between the different group of d orbitals become smaller. Therefore, the band gaps between $d_{3z^2-r^2}$ and $d_{x^2-y^2} \pm id_{2xy}$ in the collinear magnetic calculations are 395.4 , 268.1 and 159.8 meV for FeCl_2 , FeBr_2 and FeI_2 , respectively. As

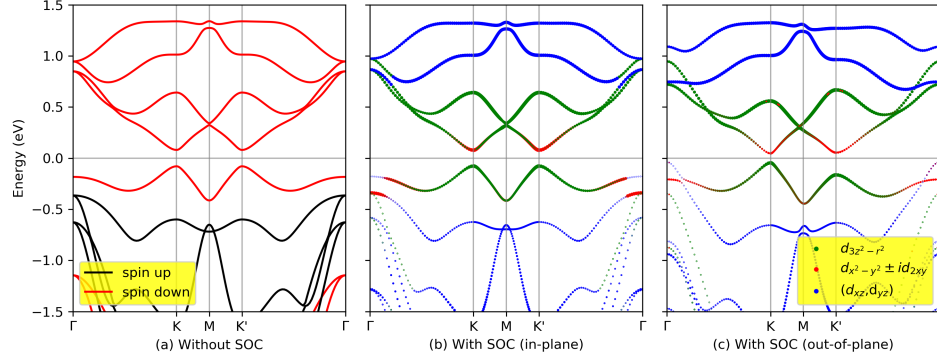


FIG. 2. The band structures of FeI₂: (a) collinear magnetic state (without SOC); (b) in-plane noncollinear magnetic state (with SOC); (c) out-of-plane noncollinear magnetic state (with SOC).

the space group of 2H FeX₂ monolayer is $P\bar{6}m2$, the generators of this space group are C_{3z} (three-fold rotational symmetry along the z direction), m_z (out-of-plane mirror symmetry) and m_{110} (in-plane mirror symmetry). The in-plane noncollinear magnetization preserves the symmetry, so the energy of in-plane noncollinear magnetic calculations along K-M and M-K' keep almost degeneracy which results in the same band gaps at K and K', see Figs. 2(b), S2(b) and S3(b). While the out-of-plane noncollinear magnetization violates the m_z symmetry, the degeneracy along K-M and M-K' are broken and the band gaps at K and K' have different values as shown in Figs. 2(c), S2(c), S3(c) and Table I. The average band gaps of out-of-plane magnetization at K and K' are about the same as that of in-plane magnetization. On the other hand, different SOC strength of halogen atoms brings about the change of band gaps (δ) as 1.0, 1.7 and 4.3 meV for FeCl₂, FeBr₂ and FeI₂, respectively (see Table I).

Here, the Wannier orbitals are projected on the d orbitals in Fe atom and p orbitals in I atoms in the *ab initio* Wannier-based tight-binding methods. An external time-dependent circularly polarized light $A(t) = A(\eta \sin(\omega t), \cos(\omega t), 0)$ irradiates the FeI₂ monolayer along the z direction, where ω is the frequency, $\eta = \pm 1$ indicates the chirality of the circularly polarized light, and A is the light amplitude. By minimal coupling [45], the time-dependent tight-binding Hamiltonian becomes

$$H(k, t) = \sum_{m,n} \sum_j t_j^{mn}(t) e^{ik \cdot R_j} c_m^\dagger(k, t) c_n(k, t),$$

where $t_j^{mn}(t) = t_j^{mn} e^{i \frac{e}{\hbar} A(t) \cdot d_j^{mn}}$ with t_j^{mn} is the hopping term, R_j is the lattice vector in the j -cell, and d_j^{mn} is the position vector between two Wannier orbitals m and n . According to Floquet-Bloch theory [43, 45, 46], an effective static Hamiltonian can be

$$H_F(k) = \sum_{m,n} \sum_{\alpha,\beta} [h_{\alpha-\beta}^{mn}(k) + \alpha \hbar \omega \delta_{mn} \delta_{\alpha\beta}] c_{\alpha m}^\dagger(k) c_{\beta n}(k),$$

$$h_{\alpha-\beta}^{mn} = \sum_j t_j^{mn} \cdot \frac{1}{T} \int_0^T dt e^{i[\frac{e}{\hbar} A(t) \cdot d_j^{mn} + (\alpha-\beta)\omega t]} \cdot e^{ik \cdot R_j},$$

where $\hbar\omega = 8\text{eV}$, $\alpha - \beta = \pm 1$ is good enough for the converged results in our work.

As shown in Fig. 3, the Floquet-Bloch band structures of out-of-plane magnetization behave differently under different chirality of circularly polarized light. As the amplitude A increases, the circularly polarized light will induce gap closing and opening at the K and K' points. Under irradiation of left circularly polarized light, as eA/\hbar increases to about 0.486 \AA , the first gap closing at K point appears as shown in Fig. 3(b); as eA/\hbar increases to about 0.607 \AA , the gap at K point enlarges, but the gap at the K' point closes as shown in Fig. 3(d); then as eA/\hbar increases further, both of the gaps at the K and K' enlarges as shown in Fig. 3(e). For right circularly polarized light, the first gap closing appears at K point when $eA/\hbar = 0.478 \text{ \AA}$ (Fig. 3(g)), and the second gap closing appears at K' point when $eA/\hbar = 0.55 \text{ \AA}$ (Fig. 3(i)) which is less than that of left circularly polarized light. Different from the out-of-plane magnetization where the degeneracy of band energies are broken at K and K' point, the response to the time-dependent left or right circularly polarized light of the in-plane magnetization behave similarly at K or K' point as shown in Fig. S4. Under irradiation of left (right) circularly polarized light, the first gap closing appears at K' (K) point when $eA/\hbar = 0.55 \text{ \AA}$ as shown in Fig. S4 (b) (Fig. S4 (g)), and the second gap closing appears at K (K') when $eA/\hbar = 0.57 \text{ \AA}$ as shown in Fig. S4 (d) (Fig. S4 (i)).

Gap closing and opening always indicate topological phase transition which is complementary to the Landau symmetry broken theory [5, 6]. Bulk-edge correspondence is an important reflection of topological phases, e.g., nontrivial edge states will appear on the edges of nanoribbons of 2D topological materials. According to the above discussions on the Floquet-Bloch band structures, there are two gap closings as the light amplitude increases. Under the irradiation of right circularly polarized light and for out-of-plane magnetization, we choose

Structures	$a/\text{\AA}$	$h/\text{\AA}$	$d/\text{\AA}$	$\Delta E_{col}/\text{meV}$	$\Delta E_{ncol}^{in}/\text{meV}$	δ/meV	$\Delta E_{ncol}^{out}/\text{meV}$
FeCl ₂	3.364	1.534	2.475	395.4	394.4	1.0	347.3(K) 452.5(K')
FeBr ₂	3.570	1.639	2.633	268.1	266.4	1.7	207.1(K) 330.0(K')
FeI ₂	3.867	1.767	2.847	159.8	155.5	4.3	92.1(K) 217.6(K')

Table I. The structural and electronic parameters of FeX₂. a is the optimized lattice constant, h is the height of the FeX₂ monolayer, d is the Fe-X bond length, ΔE_{col} is the band gap of the collinear magnetization, ΔE_{ncol}^{in} is the band gap of the in-plane noncollinear magnetization, δ is the difference between ΔE_{col} and ΔE_{ncol}^{in} , and ΔE_{ncol}^{out} is the band gap of the out-of-plane noncollinear magnetization at K and K' points.

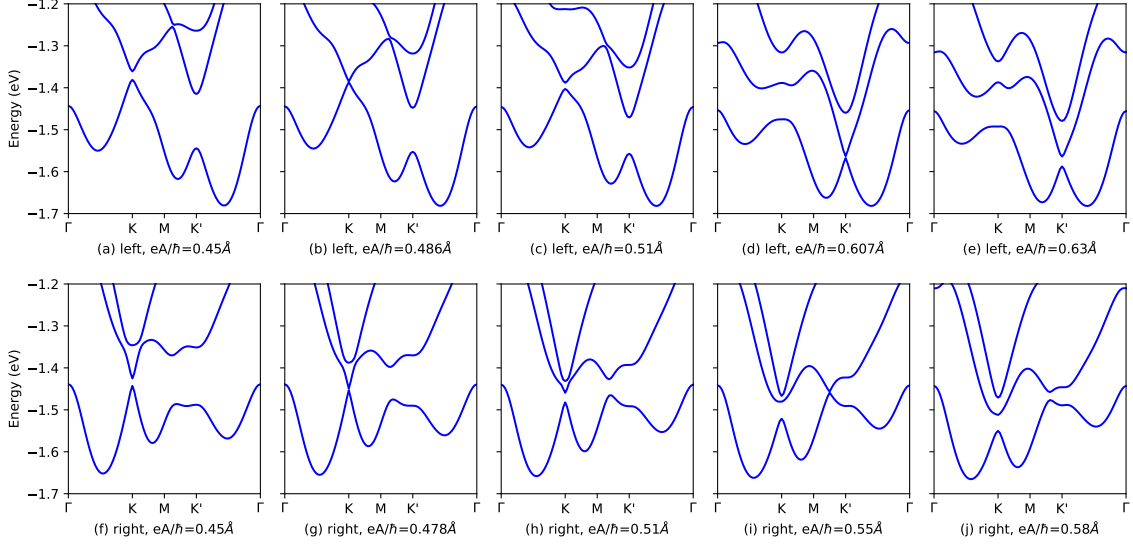


FIG. 3. The Floquet-Bloch band structures of FeI₂ with out-of-plane magnetization under the irradiation of (a)-(e) left and (f)-(j) right circularly polarized light.

$eA/\hbar = 0.45\text{\AA}$, 0.51\AA , and 0.58\AA for the slab and edge states calculations as shown in Fig. 4. Before the first gap closing, there are trivial edge states appearing in the gap between the valence and conduction bands as shown in Fig. 4(a); one of the edge states connects only the conduction (valence) bands on the left (right) edge as shown in Fig. 4(b) or (c), which indicates the trivial properties of the edge states. After the first gap closing at K point when $eA/\hbar = 0.51\text{\AA}$, two counterpropagating nontrivial edge states could be observed in Fig. 4(d); there is one left (right) propagating nontrivial edge state connecting valence and conduction bands on the left (right) edge as shown in Fig. 4(e) (Fig. 4(f)). Surprisingly, after the second gap closing at K' point, one additional nontrivial edge state appears on each edge as shown in Fig. 4(g), which indicates the transition between two different nontrivial topological phases. On the other hand, the propagating direction of two nontrivial edge states on each edge is reversed from that of topological phase with one nontrivial edge as shown in Figs. 4(h) and (i). Under the irradiation of left circularly polarized light and for out-of-plane magnetization, trivial and nontrivial edge states appear on the edge of the monolayer before and after the

gap closing as shown in Figs. S5(a)-(f), which is similar with that of out-of-plane magnetization; but because the gap at K and K' point appear at rather large energy ranges, the edge states annihilate in the bulk states as shown in Figs. S5(g)-(i). As for the in-plane magnetization (Figs. S6 and S7) under both chirality of circularly polarized light, after the first gap closing, there are nontrivial edge states appearing; but after the second gap closing, nontrivial edge states no longer appear, and a phase transition from nontrivial to trivial happens which is quite different from that of out-of-plane magnetization.

IV. CONCLUSIONS

The stable 2H FeX₂ (X=Cl, Br, I) monolayers and their intrinsic ferromagnetism enrich the family of magnetic materials, having the flexible controllability inherent to 2D magnetic materials. The semiconducting properties have potential applications in spintronics. Based on *ab initio* Wannier-based tight-binding methods, we fully capture the electronic band structural details of 2H FeI₂ monolayer and investigate the Floquet-Bloch

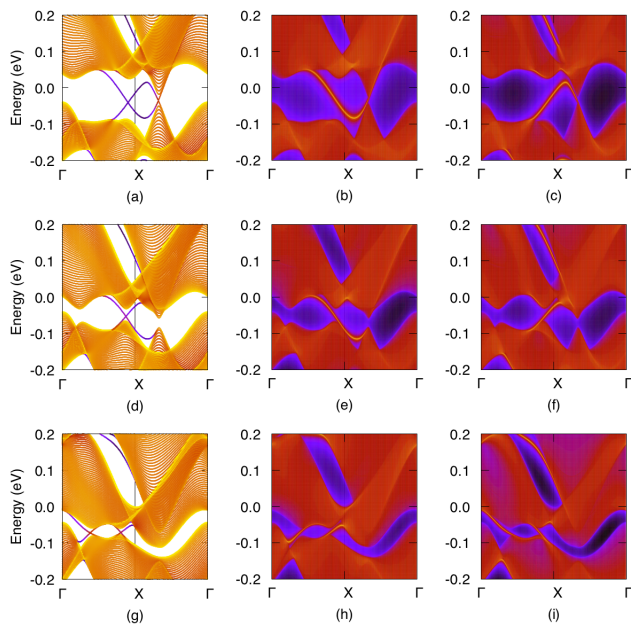


FIG. 4. The energy spectrum of FeI_2 with out-of-plane magnetization under the irradiation of right circularly polarized light for slab and edge states calculations. (a)-(c) $eA/\hbar = 0.45\text{\AA}$, (d)-(f) $eA/\hbar = 0.51\text{\AA}$ and (g)-(i) $eA/\hbar = 0.58\text{\AA}$. The left column shows the slab calculations, the middle column shows the left edge states calculations and the right column shows the right edge states calculations.

states by Floquet-Bloch theory. Left and right circularly polarized light for in-plane and out-of-plane magnetiza-

tion were considered, resulting in different physics. The Floquet-Bloch band structures demonstrate the light-induced band gap closing and opening. According to the bulk-edge correspondence, chiral edge states appear at the edges of 2D nanoribbons. More interestingly, under the irradiation of right circularly polarized light and for out-of-plane magnetization, the increasing light amplitude will not only induce a phase transition from trivial to one nontrivial chiral edge states, but also induce a topological phase transition with the number of chiral edge states from one to two. The interesting phenomena in 2H FeX_2 monolayers hold the promise for future applications such as in topological quantum computation.

ACKNOWLEDGMENTS

This work was supported by Ministry of Science and Technology of China (MOST) (Grant No. 2016YFA0301604), National Natural Science Foundation of China (NSFC) (No. 11574008, 11761161003, 11825401, and 11921005), Strategic Priority Research Program of Chinese Academy of Science (Grant No. XDB28000000), the Fonds voor Wetenschappelijk Onderzoek (FWO-VI), and the FLAG-ERA Project TRANS 2D TMD. The computational resources and services used in this work were provided by the VSC (Flemish Supercomputer Center), funded by the Research Foundation - Flanders (FWO) and the Flemish Government - department EW1, and the National Supercomputing Center in Tianjin, funded by the Collaborative Innovation Center of Quantum Matter.

-
- [1] K. v. Klitzing, G. Dorda, and M. Pepper, *Phys. Rev. Lett.* **45**, 494 (1980).
 - [2] D. J. Thouless, M. Kohmoto, M. P. Nightingale, and M. den Nijs, *Phys. Rev. Lett.* **49**, 405 (1982).
 - [3] C. L. Kane and E. J. Mele, *Phys. Rev. Lett.* **95**, 226801 (2005).
 - [4] B. A. Bernevig and S.-C. Zhang, *Phys. Rev. Lett.* **96**, 106802 (2006).
 - [5] M. Z. Hasan and C. L. Kane, *Rev. Mod. Phys.* **82**, 3045 (2010).
 - [6] X.-L. Qi and S.-C. Zhang, *Rev. Mod. Phys.* **83**, 1057 (2011).
 - [7] F. D. M. Haldane, *Phys. Rev. Lett.* **61**, 2015 (1988).
 - [8] C.-Z. Chang, J. Zhang, X. Feng, J. Shen, Z. Zhang, M. Guo, K. Li, Y. Ou, P. Wei, L.-L. Wang, Z.-Q. Ji, Y. Feng, S. Ji, X. Chen, J. Jia, X. Dai, Z. Fang, S.-C. Zhang, K. He, Y. Wang, L. Lu, X.-C. Ma, and Q.-K. Xue, *Science* **340**, 167 (2013).
 - [9] A. Bansil, H. Lin, and T. Das, *Rev. Mod. Phys.* **88**, 021004 (2016).
 - [10] L. Kou, Y. Ma, Z. Sun, T. Heine, and C. Chen, *J. Phys. Chem. Lett.* **8**, 1905 (2017).
 - [11] R. Liu, J.-J. Bi, Z. Xie, K. Yin, D. Wang, G.-P. Zhang, D. Xiang, C.-K. Wang, and Z.-L. Li, *Phys. Rev. Applied* **9**, 054023 (2018).
 - [12] Q. L. He, L. Pan, A. L. Stern, E. C. Burks, X. Che, G. Yin, J. Wang, B. Lian, Q. Zhou, E. S. Choi, K. Murata, X. Kou, Z. Chen, T. Nie, Q. Shao, Y. Fan, S.-C. Zhang, K. Liu, J. Xia, and K. L. Wang, *Science* **357**, 294 (2017).
 - [13] C. Nayak, S. H. Simon, A. Stern, M. Freedman, and S. Das Sarma, *Rev. Mod. Phys.* **80**, 1083 (2008).
 - [14] J. Alicea, *Rep. Prog. Phys.* **75**, 076501 (2012).
 - [15] X.-J. Liu, C. L. M. Wong, and K. T. Law, *Phys. Rev. X* **4**, 021018 (2014).
 - [16] C. Chan, L. Zhang, T. F. J. Poon, Y.-P. He, Y.-Q. Wang, and X.-J. Liu, *Phys. Rev. Lett.* **119**, 047001 (2017).
 - [17] T. Dietl and H. Ohno, *Rev. Mod. Phys.* **86**, 187 (2014).
 - [18] T. Dietl, *Nat. Mat.* **9**, 965 (2010).
 - [19] O. Gutfleisch, M. A. Willard, E. Brück, C. H. Chen, S. Sankar, and J. P. Liu, *Adv. Mat.* **23**, 821 (2011).
 - [20] S. Wolf, D. Awschalom, R. Buhrman, J. Daughton, S. Von Molnar, M. Roukes, A. Y. Chtchelkanova, and D. Treger, *Science* **294**, 1488 (2001).
 - [21] X. Kong, B. Cui, W. Zhao, J. Zhao, D. Li, and D. Liu, *Org. Electron.* **15**, 3674 (2014).
 - [22] A. H. Castro Neto, F. Guinea, N. M. R. Peres, K. S. Novoselov, and A. K. Geim, *Rev. Mod. Phys.* **81**, 109

- (2009).
- [23] K. Novoselov, A. Mishchenko, A. Carvalho, and A. C. Neto, *Science* **353**, aac9439 (2016).
 - [24] P. Miró, M. Audiffred, and T. Heine, *Chem. Soc. Rev.* **43**, 6537 (2014).
 - [25] A. J. Mannix, B. Kiraly, M. C. Hersam, and N. P. Guisinger, *Nat. Rev. Chem.* **1**, 0014 (2017).
 - [26] X. Kong, L. Li, O. Leenaerts, X.-J. Liu, and F. m. c. M. Peeters, *Phys. Rev. B* **96**, 035123 (2017).
 - [27] Q. H. Wang, K. Kalantar-Zadeh, A. Kis, J. N. Coleman, and M. S. Strano, *Nat. Nanotech.* **7**, 699 (2012).
 - [28] M. Chhowalla, H. S. Shin, G. Eda, L.-J. Li, K. P. Loh, and H. Zhang, *Nat. Chem.* **5**, 263 (2013).
 - [29] L. Li and M. Zhao, *J. Phys. Chem. C* **118**, 19129 (2014).
 - [30] X. Kong, L. Li, O. Leenaerts, W. Wang, X.-J. Liu, and F. M. Peeters, *Nanoscale* **10**, 8153 (2018).
 - [31] B. A. Bernevig, T. L. Hughes, and S.-C. Zhang, *Science* **314**, 1757 (2006).
 - [32] M. König, S. Wiedmann, C. Brüne, A. Roth, H. Buhmann, L. W. Molenkamp, X.-L. Qi, and S.-C. Zhang, *Science* **318**, 766 (2007).
 - [33] M. Zhao, X. Zhang, and L. Li, *Sci. Rep.* **5**, 16108 (2015).
 - [34] L. Zhang, L. Zhang, S. Niu, and X.-J. Liu, *Sci. Bull.* **63**, 1385 (2018).
 - [35] M. Claassen, C. Jia, B. Moritz, and T. P. Devereaux, *Nat. Comm.* **7**, 13074 (2016).
 - [36] Y. Wang, H. Steinberg, P. Jarillo-Herrero, and N. Gedik, *Science* **342**, 453 (2013).
 - [37] F. Mahmood, C.-K. Chan, Z. Alpichshev, D. Gardner, Y. Lee, P. A. Lee, and N. Gedik, *Nat. Phys.* **12**, 306 (2016).
 - [38] N. H. Lindner, G. Refael, and V. Galitski, *Nat. Phys.* **7**, 490 (2011).
 - [39] J. R. Schaibley, H. Yu, G. Clark, P. Rivera, J. S. Ross, K. L. Seyler, W. Yao, and X. Xu, *Nat. Rev. Mat.* **1**, 16055 (2016).
 - [40] E. J. Sie, J. W. McIver, Y.-H. Lee, L. Fu, J. Kong, and N. Gedik, *Nat. Mat.* **14**, 290 (2014).
 - [41] U. De Giovannini, H. Hübener, and A. Rubio, *Nano Lett.* **16**, 7993 (2016).
 - [42] M. Sentef, M. Claassen, A. Kemper, B. Moritz, T. Oka, J. Freericks, and T. Devereaux, *Nat. Comm.* **6**, 7047 (2015).
 - [43] H. Liu, J.-T. Sun, C. Cheng, F. Liu, and S. Meng, *Phys. Rev. Lett.* **120**, 237403 (2018).
 - [44] H. Hübener, M. A. Sentef, U. De Giovannini, A. F. Kemper, and A. Rubio, *Nat. Comm.* **8**, 13940 (2017).
 - [45] A. Gómez-León and G. Platero, *Phys. Rev. Lett.* **110**, 200403 (2013).
 - [46] Z. F. Wang, Z. Liu, J. Yang, and F. Liu, *Phys. Rev. Lett.* **120**, 156406 (2018).
 - [47] T. Kitagawa, T. Oka, A. Brataas, L. Fu, and E. Demler, *Phys. Rev. B* **84**, 235108 (2011).
 - [48] G. Kresse and J. Furthmüller, *Phys. Rev. B* **54**, 11169 (1996).
 - [49] G. Kresse and D. Joubert, *Phys. Rev. B* **59**, 1758 (1999).
 - [50] P. Hohenberg and W. Kohn, *Phys. Rev.* **136**, B864 (1964).
 - [51] J. P. Perdew, K. Burke, and M. Ernzerhof, *Phys. Rev. Lett.* **77**, 3865 (1996).
 - [52] A. Togo and I. Tanaka, *Scr. Mater.* **108**, 1 (2015).
 - [53] A. A. Mostofi, J. R. Yates, G. Pizzi, Y.-S. Lee, I. Souza, D. Vanderbilt, and N. Marzari, *Comput. Phys. Commun.* **185**, 2309 (2014).
 - [54] Q. Wu, S. Zhang, H.-F. Song, M. Troyer, and A. A. Soluyanov, *Comput. Phys. Commun.* **224**, 405 (2018).
 - [55] M. L. Sancho, J. L. Sancho, J. L. Sancho, and J. Rubio, *J. Phys. F: Met. Phys.* **15**, 851 (1985).
 - [56] E. Torun, H. Sahin, S. Singh, and F. M. Peeters, *Appl. Phys. Lett.* **106**, 192404 (2015).
 - [57] M. Ashton, D. Gluhovic, S. B. Sinnott, J. Guo, D. A. Stewart, and R. G. Hennig, *Nano Lett.* **17**, 5251 (2017).